Simulation of modified Trombe wall

Jerzy Szyszka[1,*]

[1]Rzeszow University of Technology, The Faculty of Civil and Environmental Engineering and Architecture, Poznanska 2, 35-082 Rzeszow, Poland

Abstract. Passive systems are becoming increasingly popular among designers, which is reflected in their frequent use in the construction of modern buildings. The prevailing material in façade design is glass which enables i.a. photothermal conversion of solar energy either in the so-called direct systems or in one of a number of the collector-and-storage Trombe wall variants. In order to estimate how the aforementioned passive solutions affect the energy balance of a building, the efficiency of such solutions needs to be determined first. This paper presents the research proposal that would use a simple-structure laboratory simulator. The proposed method is based on the analogy of supplying heat into the TW itself with an internal heat source. In order to simulate the absorption of solar radiation that takes place in the absorber, the heat was produced by the heating cable embedded in such an absorber. The results of tests carried out according to one of the Design of Experiments (DOE) methods enabled the development of an empirical model showing the operation efficiency of the originally modified Trombe wall.

1 Introduction

A classic Trombe wall (TW) is a partition consisting of a masonry wall (the so-called core), and a glazing. The glazing, due to its selective properties, can pass through a short-wave high energy solar radiation to the outer surface of the masonry wall (absorber), while limiting the heat transfer. The photothermal conversion of solar radiation takes place on the absorber. The heat supplied in this way is stored in the wall and transferred to the interior of the building. The efficiency with which TW uses the transferred heat may vary depending on thermophysical parameters and climatic conditions. It is mostly determined with the use of numerical models that are based either on the finite element method FEM or finite difference method DEM [1–3]. In the papers [4, 5], the calculation of the efficiency of various types of walls was carried out in field conditions either with the use of specially-prepared research chambers or experimental houses [6]. The latter ones, in relation to numerical methods, are free of errors that could result from the simplifications adopted in the mathematical description. However, they do refer to local climatic conditions. Therefore, the resulting conclusions do not allow for developing a universal empirical model which would enable the estimation of the wall thermal balance either in different climatic conditions or with a modified configuration.

* Corresponding author: jszyszka@prz.edu.pl

The laboratory simulators [7–8] may prove to be an alternative to the field research. The tests carried out with their use enable not only the development of a statistical model, but also an assessment of its adequacy. A method based on the DOE (Design of Experiment) theory [10] is an excellent tool for the said purpose. Conducting the research with preset air temperature differences on opposite sides of the tested wall is not a major problem. A freezer chamber may be used for this purpose. However, the simulation of solar radiation which heats the wall's absorber from the outside is quite problematic. The application of lamps that are used for testing solar collectors or photovoltaic cells proves ineffective in the case of passive walls. The necessity to reproduce the characteristics of a wavelength that allows for the transmission of the emitted energy through the glazing in a similar manner to the characteristics of the AM2 spectrum requires the use of huge power lamps. In this case, if we choose to observe the wall model subjected to low, including negative, air temperatures from the outside of the tested wall, providing the energy at the level of 1,000 W/m^2 would require significant power of cooling aggregates [11–12]. For example, a simulator for the AM2 atmosphere optical mass, located at the Institute of Heat Engineering of the Warsaw University of Technology, requires the energy consumption of 24,000 W [13] in order to produce the radiation intensity of 740 W/m^2. For this reason, the said method is irrational in the case of testing the Trombe wall in a near-real scale. The method proposed in this paper is based on the analogy of supplying heat into the TW itself with an internal heat source. In order to simulate the absorption of solar radiation that takes place in the absorber, the heat was produced by the heating cable embedded in such an absorber (figure 1.).

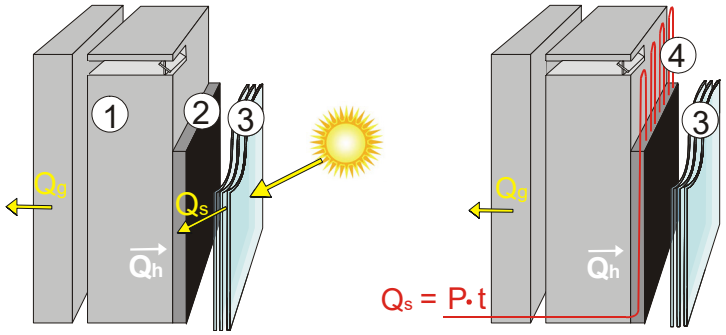

Fig. 1. Diagram showing the heating of the Trombe wall with: a) solar radiation, b) heating cable; 1–masonry part of the wall (core), 2–absorber, 3–glazing, 4–heating cable, Q_h–heat losses, Q_g–gain energy, Q_s –heat supplied by the sun's radiation.

The thermal operation of the TW can be reduced to superposition of two states. The first one concerns functioning in the periods of low solar radiation or its absence in the night hours. In this case, over time t, the wall generates heat losses (1):

$$Q_h = A \cdot \frac{\Delta T \cdot t}{R_T} = \Delta T \cdot \int q_h dt \tag{1}$$

where:

Q_h – heat losses through the wall over time t, caused by the difference of air temperature $\Delta T=(T_i-T_e)$ on both sides of the wall,

R_T – total thermal resistance of the wall,

q_h – heat flux density through the wall, caused by the difference of air temperature $\Delta T=(T_i-T_e)$ on both sides of the wall.

The second operational variant is related to the impact that solar radiation has on the wall. The heat supplied to the absorber of wall heat Q_s can be calculated from the following formula (2):

$$Q_s = A \cdot \int (g \cdot \alpha \cdot I_i \cdot s) dt \tag{2}$$

where:
I_i – solar irradiance[W/m^2],
A – glazed area [m^2],
g – solar gain factor,
s – shadow factor,
α – absorbing capacity of the wall surface (α=0.95).

Calculating the amount of heat supplied to the absorber of the wall (eq. 2) is relatively simple, but determination of the effective gains Q_g that improve its heat balance is more complicated. Their value is affected by the additional - in relation to the ones specified in the equation (eq. 1) - heat losses related to the increase in the energy level of the wall. They can be represented in the form of a distribution efficiency factor η_d of the absorbed heat (3):

$$\eta_d = \frac{Q_g}{Q_s} = \frac{\int (q_i - q_h) dt}{Q_s} \tag{3}$$

where:
q_i – heat flux density measured on the inner surface of the wall.

The aim of the research described in this paper was to determine the η_d coefficient for the selected material solutions as a function of the adopted boundary (climatic) conditions of the modified Trombe wall prototype (slotted collector-accumulation wall, CAW). The solution aims for improving the efficiency of heat distribution, as compared to the classic solution, by the use of internal air circulation [8, 9]. For this purpose, the core of the wall was divided into two parts. The resulting gap was connected with the space between the absorber and the glazing with the use of channels located in the lower and upper part of the masonry (figure 2). The said channels could be closed with the use of automatic throttles and their function was to cause a selective heat flow. The opening of such throttles while the wall was being heated up made the wall warmer (from the inside) with the circulating warm air. Closing the throttles at night reduced heat losses.

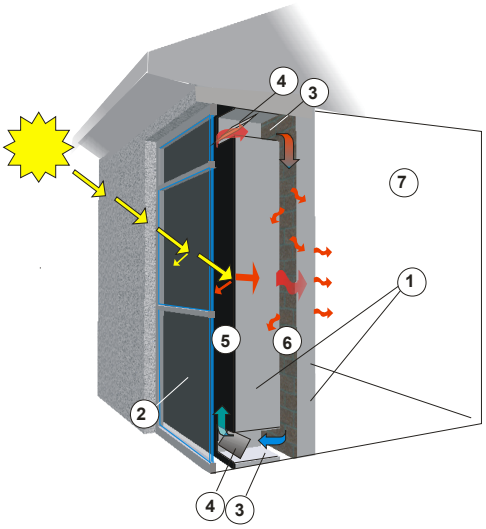

Fig. 2. Slotted collector-accumulation wall (CAW): 1–masonry wall consisting of two parts, 2–transparent collector cover, 3–circulation channel, 4–automatic throttles, 5–air space between the glazing and the absorber (outer slot), 6–inner slot, 7–utility room.

The slotted collector-accumulation wall prototype (Polish abbrev.: SPKA) uses modern glass panes: a double-chamber glass pane with a heat transfer coefficient U_g = 0.6 W/m^{2}K with capacity to transmit solar radiation energy (solar gain factor) g = 0.59, as well as a single-chamber glass pane with a coefficient U_g = 1.2 W/m^{2}K with capacity to transmit solar radiation energy g = 0.64.

2 Materials and Methods

2.1 Description of the simulator used for slotted collector-accumulation wall research

The tests of the distribution of heat transferred to the wall, with different air temperatures on its opposite sides, were carried out in a specially prepared simulator, the conceptual design and cross-section of which are shown in figure 3.

The site consists of two chambers – a “cold chamber” and a “heat chamber”, between which the modified Trombe wall models were built in. The internal dimensions of the simulator h=250 cm, b=350 cm allowed for installing and conducting simultaneous tests on three wall models measuring 100 cm x 210 cm. The function of the “cold” chamber was to simulate the impact of the outside air in winter conditions on the outer surface of the wall. The “heat” chamber imitated the impact of internal conditions of the building on the inner surface of the wall.

In order to simulate the heat flux coming from the absorbed solar radiation, a mineral insulated 50 W/mb constant-resistance Raychem EM-MI heating cable was used, and it was embedded in the plaster of the absorption layer. The heating cable was connected to the 230 V power supply via a TAR1.6 laboratory-type control autotransformer. The reduction of the heating cable power made it possible to simulate the absorption of variable solar irradiance. The amount of energy supplied to the heating cable was monitored and registered by an electronic energy consumption recorder: Voltcraft Energy Logger 4000, with the accuracy class of ± 1%.

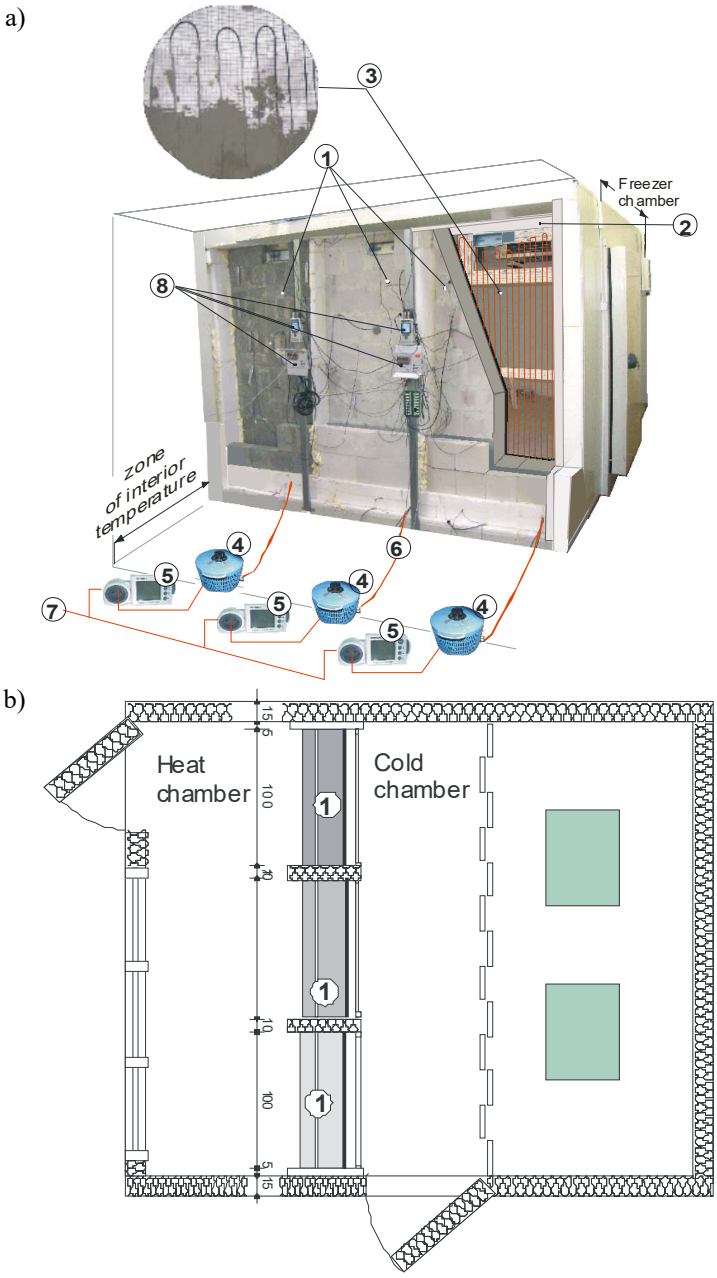

Fig. 3. Simulator used for the research: a) conceptual design, b) horizontal cross-section; 1–analyzed CAW walls, 2–frame with glazing, 3–Raychem EM-MI heating cable embedded in the absorber, 4–autotransformer, 5–instrument recording the energy consumption, 6–cable supplying power to the heating cable, 7–230V power cable.

2.2 Materials used to build the wall models

The research in the simulator was carried out simultaneously for three types of CAW differing in the masonry material used to make the masonry wall: ordinary concrete on

natural aggregate (ρ=2200 kg/m^3), aerated concrete (ρ=750 kg/m^3) and sand-lime blocks (ρ=1600 kg/m^3). Simultaneous measurement of the tested parameters in three types of partitions provided similar boundary conditions for the experiment. The tested partitions were thermally isolated both from each other and from the simulator housing with the use of spacers made of Styrofoam and Spaceloft aerogel mat.

2.3 Determination of boundary conditions and simulation variables

The aim of the research was to determine the heat distribution efficiency η_d (eq.4). The impact of boundary conditions on η_d was limited to the outdoor air temperature T_e and the amount of the supplied heat Q_s (eq.2) for a selected wall material configuration, assuming a constant level of air temperature inside the building of T_i = 20°C.

$$\eta_d = f(T_e, Q_s) \tag{4}$$

The actual (observed) gains Q_i obtained from heating the absorber were expressed as an integral from the heat flux density q_i observed on the inner surface of the wall, caused by the supply of a specific portion of heat to the absorber through the heating cable (Fig. 4, eq.3).

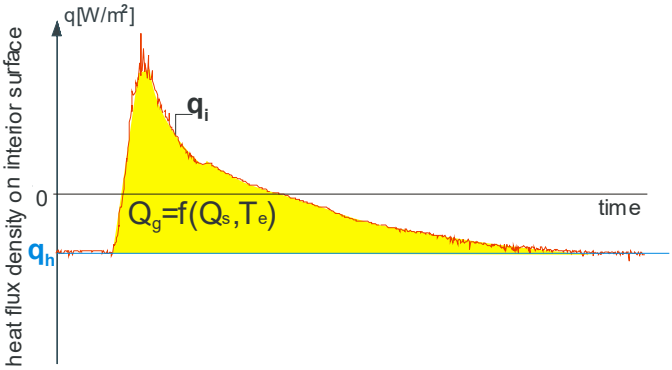

Fig. 4. Change in the heat flux density on the inner wall surface caused by heating the absorber.

2.4 Experimental design

The Design of Experiments module available in STATISTICA software allows for modelling the process of new experiments, the results of which - after the actual execution of the planned experiment - are subjected to a comprehensive statistical analysis. The described experiment included the construction of a model that would enable finding the connections between the selected parameters (temperature, heating power and time) and the efficiency of η_d distribution in the tested solutions. The Response Surface Methodology (RSM) method implemented in STATISTICA software was used for the said purpose, with a selected central composition plan [14–15]. Such a plan is one of the most popular forms of RSM due to its efficiency and possibility to limit the number of necessary experiments, while meeting the criteria of implementation, effectiveness and informativeness. In this case, the tests are carried out according to the imposed scheme that determines the number of input values combinations in the adopted variation ranges. Experimental designs require both the input data and the output parameter described by the response surface to be standardized. It results in the necessity to express the input values variation ranges in

a standardized form. This is achieved by introducing the so-called standardization function at the very beginning, and, at the stage of evaluating the results – the de standardization of the input values. The variation range of these variables corresponds to the dimensionless values standardized in the range <-1;1>. Their distribution from the so-called center point is additionally determined by the value of the star point distance α.

Three input variables were adopted in the conducted experiment: change of outside air temperature T_e, instantaneous power of the heating cable P and the heating time t. The variation range of input variables was determined based on the climate database for Poland during the heating season. It was assumed that the outside air temperature would change from -17.9°C to 7.9°C. The simulation of heat Q_s supplied to the absorber in accordance with eq2. with the use of the heating cable was expressed as the product of the instantaneous power of the absorber heating cable P and the heating time t. The P and t values determined in relation to the experimental design, after taking into account the surface of the wall model ($2m^2$) in which the cable was embedded, are summarized in Table 1. The adoption of three input quantities and five intermediate points (-1,-α,0,+α,+1) (table 1) required 16 series of tests for each of the adopted material configurations. In the case of a full-ended design, that would cover the studies of all possible interactions, the number would be 5^3=125. The list of the standardized values and the corresponding actual values of independent variables are presented in table 1.

Table 1. The central orthogonal compositional plan adopted for the research.

Configuration no.	Standardized values of input independent variables			Actual values of the input independent variables		
	Te	P	t	Te [C]	P [W]	t [h]
1	0	0	-α	-5.0	500.0	3.7
2	-1	+1	-1	-15.0	800.0	4.0
3	-1	-1	-1	-15.0	200.0	4.0
4	1	+1	-1	5.0	800.0	4.0
5	1	-1	-1	5.0	200.0	4.0
6	-α	0	0	-17.9	500.0	5.0
7	0	+α	0	-5.0	886.2	5.0
8	0	-α	0	-5.0	113.8	5.0
9 (c)	0	0	0	-5.0	500.0	5.0
10 (c)	0	0	0	-5.0	500.0	5.0
11	+α	0	0	7.9	500.0	5.0
12	-1	-1	+1	-15.0	200.0	6.0
13	-1	+1	+1	-15.0	800.0	6.0
14	+1	-1	+1	5.0	200.0	6.0
15	+1	+1	+1	5.0	800.0	6.0
16	-0	0	+α	-5.0	500.0	6.3

2.5 Performing the simulation

The tests consisted in recording the temperature values and heat flux density both on the internal wall surface q_g and in the adopted sections of the slotted collector-accumulation walls, the operation of which, in conditions determined by the experimental design (table 1), was controlled with the use of a laboratory simulator (figure 2). A single study was conducted from the steady state q_h, connected with the adopted temperature gradient (T_i-T_e) on both sides of the wall, by observing the change in the heat flux density q_h as a result of heating the absorber to the steady-state q_h. The time of a single test was up to 120 hours.

Based on the data collected for each of the considered material configurations, the distribution efficiency was calculated in accordance with the following formula (5):

$$\eta_d = \frac{\int (q_i - q_h)dt}{P \cdot t} \tag{5}$$

where:
q_i – heat flux density measured on the inner surface of the wall, after the absorber has been heated up with the cable with power P over time t,
q_h – heat flux density determined on the inner wall surface observed in steady-state conditions for the temperature T_e.

The functional dependencies (response surfaces) were determined for the obtained relations between the distribution efficiency η_d and independent variables (T_e, P, t) with the use of STATISTICA software [10]. Then statistical evaluation of the significance of individual input variables, their interactions, as well as the adequacy of the functional model for measurement data were carried out for such functional dependencies.

3 Results and discussion

The analysis of the significance of independent variables together with the adequacy test of the response surface function showed the statistical significance of P(t) and T_e variables on predicting the efficiency η_d. The significance level p of the function coefficients, with the mentioned variables, reached the value lower than 0.05. The variable t in each of the considered configurations in the adopted field of experiment turned out to be statistically irrelevant. The slight differences in the coefficient values of T_e and P variables did not give a basis for determining which one of them has a dominant impact on estimating the distribution efficiency.

Table 2. Comparison of distribution coefficient equations as a function of external air temperature and instantaneous power of the heating cable.

Type of the slotted CAW (SPKA)	Coefficient of determination R^2 / Standard estimation error	Response surface equation
Plain concrete, double-chamber glass pane	0.90 / 3.25	$\eta_{d\_CUg06} = 56.055 + 0.67 \cdot T_e + 0.018 \cdot P$ Eq.5
Aerated concrete double-chamber glass pane	0.94 / 1.33	$\eta_{d\_ACUg06} = 32.644 + 0.389 \cdot T_e + 0.013 \cdot P$ Eq.78
Silica, double-chamber glass pane	0.95 / 1.54	$\eta_{d\_CSUg06} = 49.98 + 0.547 \cdot T_e + 0.044 \cdot P$ - $+ 2.75 \cdot 10^{-5} \cdot P^2 - 3.73 \cdot 10^{-4} \cdot T_e \cdot P$ Eq.8

The applicability range of the equations (eq.5-eq.8, tab. 2) for the distribution efficiency coefficient is limited to the domain of an experiment within the changeability range of independent variables.

4 Conclusions

- The presented method which uses a simple-structure simulator provides great opportunities for developing an empirical model to assess the efficiency of passive systems, such as the Trombe wall.
- The use of the design of experiment theory implemented in the DOE module of Statistica software makes it possible to limit the number of tests required to assess the statistical compatibility of the obtained model to the observed data.
- The elaborated distribution efficiency equations, after performing simple transformations of the η_d function of the variable P (heating cable power) to the function of the variable Is (solar irradiance), allow for estimating the wall balance for the selected climatic data configuration in the domain of the experiment.
- Among the considered independent variables, both the outside air temperature and the instantaneous power of the heating cable (solar irradiance) had a statistically significant impact on the distribution coefficient value.
- The impact of the outside air temperature on the efficiency may be connected with the output energy level of the wall that is dependent on such temperature. The lower the average wall temperature, the more of the supplied heat is used to raise the temperature of the wall to the level at which the direction of the heat flow changes, resulting in some gains.
- The impact of the outside air temperature on the distribution efficiency may be connected with absorber heat losses through the glazing. They are proportional to the difference in temperatures between the outdoor air and the absorber surface.
- The impact of wind, omitted in the simulations, can be taken into account by adequately reducing the outside air temperature to the level at which the temperature on the outer surface of the glazing reaches the same value as when the wind blows at a certain speed.

References

1. J. Shen, S. Lassue, L. Zalewski, D. Huang, Energ. Buildings, **39**, 962–974 (2007)
2. J. Shen, S. Lassue, L. Zalewski, D. Huang, Journal of Thermal Science, **16**, 46–55 (2007)
3. P. Ochab, W. Kokoszka, J. Kogut, I. Skrzypczak, J. Szyszka and A. Starakiewicz, IOP Conf. Ser.: Earth Environ. Sci. **95** 042017 (2017)
4. F. Abbassi, L. Dejmani, Energ. Buildings, **105**, 119–128 (2015)
5. F. Abbassi, N. Dimassi, L. Dejmani, Energ. Buildings, **80**, 302–308 (2014)
6. L. Laskowski, *Ochrona cieplna i charakterystyka energetyczna budynku*, (Oficyna Wydawnicza Politechniki Warszawskiej, Warszawa, 2001)
7. G. Zhou, M. Pang, Energy **93,** 758–769 (2015)
8. J. Szyszka, J. Kogut, I. Skrzypczak, W. Kokoszka, IOP Conf. Ser.: Earth Environ. Sci. **95**, 042018 (2017)
9. L.Licholai, J.Szyszka, PL Patent, PL408488–A1(2014-06-09)
10. STATISTICA, StatSoft Polska Sp. z o.o., www.statsoft.pl {accessed 2018-01-25}
11. http://www.solar.seric.co.jp/ {accessed 2018-01-25}
12. http://www.dlr.de {accessed 2018-01-25}
13. D. Chwieduk, *Energetyka słoneczna budynku*, (Arkady, Warszawa, 2011)
14. J. Konkol, G. Prokopski, Constr. Build. Mater. **123**, 638–648 (2016)
15. L. Lichołai, B. Dębska, Arch. Civil Mech. Eng. **14**, 466–475 (2014)